Beclin-1 deficiency in the murine ovary results in the reduction of progesterone production to promote preterm labor

Thomas R. Gawriluk[a], CheMyong Ko[b], Xiaoman Hong[c], Lane K. Christenson[c], and Edmund B. Rucker III[a,1]

[a]Department of Biology, University of Kentucky, Lexington, KY 40506; [b]Department of Comparative Biosciences, University of Illinois at Urbana–Champaign, Urbana, IL 61802; and [c]Department of Molecular and Integrative Physiology, University of Kansas Medical Center, Kansas City, KS 66160

Edited by R. Michael Roberts, University of Missouri, Columbia, MO, and approved August 21, 2014 (received for review May 19, 2014)

Autophagy is an important cellular process that serves as a companion pathway to the ubiquitin-proteasome system to degrade long-lived proteins and organelles to maintain cell homeostasis. Although initially characterized in yeast, autophagy is being realized as an important regulator of development and disease in mammals. *Beclin1* (*Becn1*) is a putative tumor suppressor gene that has been shown to undergo a loss of heterozygosity in 40–75% of human breast, ovarian, and prostate cancers. Because *Becn1* is a key regulator of autophagy, we sought to investigate its role in female reproduction by using a conditional knockout approach in mice. We find that pregnant females lacking *Becn1* in the ovarian granulosa cell population have a defect in progesterone production and a subsequent preterm labor phenotype. Luteal cells in this model exhibit defective autophagy and a failure to accumulate lipid droplets needed for steroidogenesis. Collectively, we show that *Becn1* provides essential functions in the ovary that are essential for mammalian reproduction.

Autophagy is an evolutionarily conserved cellular process from yeast to mammals that recycles long-lived proteins and organelles to maintain cell energy homeostasis, and is classically activated through the nutrient sensor, mammalian target of rapamycin complex (1–3). Cellular material is encapsulated within a double phospholipid bilayer organelle called the "autophagosome," which fuses with a lysosome to degrade the internalized debris. Using genetic screens in yeast, more than 34 autophagy-related (*Atg*) genes have been identified, with most having clear homologs in higher eukaryotes through protein-sequence identity (4–6). BECLIN1 (BECN1), a haploinsufficient tumor suppressor, is an essential autophagy protein that directs the initiation phase and maturation-fusion phase through its participation in two distinct phosphoinositide 3-kinase class III complexes (7–9). Autophagy is not only important for normal development, but it is linked to an array of diseases including neurodegenerative disorders, liver disease, heart disease, inflammatory diseases, and cancer (10, 11). We previously showed a role for BECN1 and autophagy in the establishment of the murine primordial follicle pools in a germ-line knockout model (12). In this study, we follow up on these results and investigate the role of BECN1 in ovarian granulosa cells.

In mammals, the success of early pregnancy from embryo implantation to development of the conceptus depends on the function of an ephemeral endocrine gland, the "corpus luteum" (CL), which rapidly forms in the ovary from the remains of the ovulated follicle and migrating somatic cells through a process called "luteinization." Progesterone is an essential hormone that acts at several different levels during pregnancy, including the development of the endometrium for implantation of the embryo and the maintenance of pregnancy through quiescence of the myometrium (13, 14). Luteal cells within the CL use cholesterol for steroidogenesis to produce progesterone and synthesize upwards of 40 mg of progesterone per day in humans (15). Cholesterol not only supports steroidogenesis, but its cellular uptake and intracellular distribution is viewed as the beginning of this series of biochemical reactions (16). Autophagy has been implicated in lipid metabolism through a process termed "lipophagy" to provide the cell with sources of triglycerides and cholesterol (17, 18), although the significance of autophagy in progesterone synthesis has never been shown.

In this study, we investigated the function of autophagy in somatic cells by using a targeted deletion approach to knockout *Becn1* in the precursor follicular granulosa cells, which ultimately terminally differentiate into the lipid-rich steroidogenic luteal cells. We show that luteal *Becn1* deficiency leads to CL, which have impaired lipid droplet formation and a marked reduction in progesterone production resulting in a preterm labor phenotype. To our knowledge, this is the first genetic study showing a role for *Becn1* during pregnancy and highlights that autophagy is necessary for fertility.

Methods

Mice. *Becn1*^{fl} (12), cytochrome P450, family 19, subfamily A, polypeptide 1 (*CYP19A1*)–codon-improved Cre recombinase (*iCre*) (19), *Amhr2*$^{tm3(cre)Bhr}$ (20), green fluorescent protein (*GFP*)–microtubule-associated protein 1A/1B-light chain 3 (*LC3*) (RIKEN no. RBRC00806) (21), and *CAG*-chloramphenicol acetyltransferase (*CAT*)-enhanced GFP (*EGFP*) (kind gift from K. Wagner, University of Nebraska Medical Center, Omaha, NE) (22) mice were all on a 129/Sv and B57BL/6 mixed background. Conditional knockout females were generated by crossing *Becn1*$^{fl/\Delta}$; *CYP19A1-iCre*$^{+}$ males to *Becn1*$^{fl/fl}$ females. Controls females were littermates that did not carry the *CYP19A1-iCre* allele. All animals were genotyped by using genomic DNA isolated from tail snips, and alleles were detected by published PCR assays (12, 19–22). All mice were housed in a University of Kentucky Division of Laboratory Animal Resources facility, subjected to a 14:10 h light:dark cycle and given food and water ad libitum. For breeding trials, 2–3 females (8-wk- to 6-mo-old) were

Significance

The success of mammalian reproduction is contingent upon the production of hormones within the female to not only promote germ cell development, but to establish and maintain pregnancy. We demonstrate that abrogating autophagy, a cellular process to maintain energy stores, can lead to reproductive defects that prevent a successful pregnancy in mice. Females that lack the crucial autophagy gene *Beclin1* (*Becn1*) in the progesterone-producing cells of the ovary demonstrate reduced circulating progesterone and a preterm birth phenotype concurrent with the loss of litters, which is rescued by the administration of exogenous progesterone. Because progesterone is a necessary hormone for mammalian pregnancy, these data suggest that autophagy may play a role in steroidogenesis and, thus, in successful human reproduction.

Author contributions: T.R.G., C.K., L.K.C., and E.B.R. designed research; T.R.G. and X.H. performed research; C.K. contributed new reagents/analytic tools; T.R.G., C.K., L.K.C., and E.B.R. analyzed data; and T.R.G. and E.B.R. wrote the paper.

The authors declare no conflict of interest.

This article is a PNAS Direct Submission.

[1]To whom correspondence should be addressed. Email: edmund.rucker@uky.edu.

placed with a single already-proven fertile C57BL/6 male, and those with a seminal plug on the following morning were separated into a new cage and this developmental stage was classified as pregnancy day 0.5 (P0.5). Starting on P10.5, the females were palpitated for fetuses to determine pregnancy status. All animal procedures were compliant under the approved University of Kentucky Institutional Animal Care and Use Committee protocol, 2008–0372.

Exogenous Progesterone Administration and Collection of Pregnant Mare's Serum Gonadotropin-Primed Granulosa Cells. For progesterone supplementation, the pregnant females were s.c. injected with progesterone (Sigma-Aldrich; P0130) dissolved sesame oil (1 mg/100 μL per day) or oil alone (control) (Sigma-Aldrich; S3547). Injections began on P10.5 at 1300 hours and continued each day until P16.5 for a total of seven injections.

Granulosa cells were collected from pregnant mare's serum gonadotropin (PMSG)-primed animals as described (19, 23). Briefly, 21- to 23-d-old mice were injected intraperitoneally (IP) with 5 IU PMSG (Calbiochem; 367222) at 1200 hours to stimulate folliculogenesis. Forty-eight hours later, ovaries were dissected out, cleaned, and incubated in sucrose/EGTA media for at least 10 min to facilitate separation into individual cells. Granulosa cells were released from the follicles by poking the follicles with a 28-gauge needle. The cell suspension was filtered through 40 μM nylon mesh to remove oocytes and primordial follicles. Granulosa cells were then pelleted, flash frozen in liquid nitrogen, and stored at −80 °C until analysis.

Tissue and Blood Collection. To control for any circadian controlled genes and/or proteins, all mice were euthanized between the hours of 1300 and 1500 on the developmental day indicated. Mice were euthanized by cervical dislocation or cardiac exsanguination via 18 gauge needle for serum analysis after being anesthetized with Avertin (0.25 mg/g body weight) by IP injection. Reproductive tracts were removed and washed briefly in ice-cold PBS and immediately processed. The ovaries were removed from their bursa and weighed. For RNA and protein analysis, the CL were dissected from the ovary and flash frozen in liquid nitrogen. For routine histology, ovaries were placed into fresh, ice-cold 4% (wt/vol) paraformaldehyde for 6–16 h. For GFP-LC3 analysis, females were first transcardally perfused (25 mL/min) with ice-cold 10% (wt/vol) sucrose for 3 min, followed by fresh 4% (wt/vol) paraformaldehyde for 5 min before removal of ovaries. The ovaries were then immersed in 4% (wt/vol) paraformaldehyde for 4 h.

For serum collections, blood collected during exsanguination was transferred to a 2-mL round-bottom tube, incubated for 90 min at room temperature to allow for clotting, and centrifuged for 15 min at 1,000 × *g*. Serum was removed and transferred to a new 1.5-mL tube and stored at −20 °C. For plasma collections, ∼50 μL of blood was collected every other day from alternating submandibular venous beds by using a 5-mm lancet (Goldenrod; Medipoint). Blood was immediately mixed with EDTA, to a final concentration of ∼0.01 M to prevent clotting, and then centrifuged for 15 min at 1,000 × *g*. Plasma was removed and transferred to a new 1.5-mL centrifuge tube and stored at −80 °C.

Tissue Preparation and Histology. For GFP-LC3 and Oil Red O analysis, frozen sections were prepared from ovaries as follows: fixed ovaries were washed with PBS (three changes, 15 min each) and cryoprotected by placing them sequentially into 10%, 20%, and 30% (wt/vol) sucrose solution until the tissue sunk. Cryoprotected tissues were blotted dry, transferred into Tissue-Tek Optimal Cutting Temperature Compound (Sakura Finetek USA), flash-frozen in an isopentane/dry-ice slurry, and stored at −80 °C until sectioned on a Leica CM1850 cryostat at 5-μm sections.

For histology and immunohistochemistry, paraffin sections were prepared as follows: fixed ovaries were washed with PBS (three changes, 15 min each) and dehydrated by transferring them through an ethanol gradient: 50% (vol/vol) for overnight, 70% (vol/vol) for storage. Processing was done by using a rapid microwave processor containing 100% ethanol for 1 h, 100% isopropanol for 1 h, vacuum dried, and infiltrated with molten paraffin for 1 h, and finally embedded into molds (Milestone Histo-5; Mikron Instruments). Sections (5 μM) were placed onto gelatin-subbed slides and stored at room temperature. Sections were deparaffinized with xylene, rehydrated, and then either stained with hematoxylin and eosin for routine analysis or processed for immunohistochemistry.

For immunofluorescence of GFP, sections were subjected to antigen retrieval by treatment with 10 mM sodium citrate at pH 6.0 and incubated at 95 °C for 20 min. The sections were washed three times with PBS, then incubated in PBS with 0.2% Triton X-100 for 20 min for membrane permeabilization, followed by three washes in PBS. The slides were blocked with 10% (wt/vol) BSA in PBS for 1 h at room temperature and then incubated with α-GFP primary antibody with 3% (wt/vol) BSA in PBS overnight at 4 °C. The following day, the slides were washed with PBS three times, incubated with diluted secondary antibody for 1 h at room temperature, washed with PBS three times, and mounted with Prolong Gold antifade media containing 4′,6-diamidino-2-phenylindole (Life Technologies; P-36931).

Oil Red O Staining. Frozen sections (5 μM) were placed onto gelatin-subbed slides and allowed to air dry for at least 1 h. The dried sections were washed in PBS to remove OCT, incubated in 60% (vol/vol) isopropyl alcohol for 5 min, stained with freshly prepared 0.15% Oil Red O for 10 min, washed in 60% (vol/vol) isopropyl alcohol, counterstained with hematoxylin, and mounted with glycerol jelly.

Hormone Profiling. All hormones were analyzed by the Ligand Assay and Analysis Core run by Center for Research in Reproduction at the University of Virginia, School of Medicine, which is funded by the National Institute of Child Health and Human Development through a U54 Center Grant (U54-HD28934). Estradiol was measured by ELISA (Calbiotech), progesterone by radioimmune assay (RIA) (Siemens), and follicle-stimulating hormone (FSH) and luteinizing hormone (LH) together by Milliplex multianalyte panels (Millipore).

Immunoblotting. Flash-frozen tissue or cells were subjected to ice-cold RIPA buffer with freshly added protease and phosphatase inhibitors (Santa Cruz; sc-24948), sonicated, rocked for 30 min at 4 °C, and centrifuged at 9,300 × *g* for 10 min at 4 °C. The soluble fraction was collected and total protein was quantified by bicinchoninic acid assay (Thermo; 23225). Twenty-five micrograms of total protein per sample was denatured in Laemmli buffer and separated by SDS/PAGE on a 12% Tris-acrylamide minigel. Granulosa cell protein extracts were first precipitated by 15% (wt/vol) trichloroacetic acid/0.02% sodium deoxychlorate to concentrate the lysate. Separated proteins were transferred to a PVDF membrane with 0.45 μM pores (GE Healthcare; RPN303F) overnight (∼16 h at 70 mV) at 4 °C. Membranes were blocked by using 5% (wt/vol) skim milk in Tris-buffered saline with Tween 20 (TBST), and diluted primary antibody was added to the membrane and incubated overnight at 4 °C. The membranes were washed three times with TBST for 5 min each and then HRP-conjugated secondary antibody diluted in 5% (wt/vol) skim milk in TBST was added and incubated for 1 h at room temperature with agitation. Then the membranes were washed three times with TBST for 5 min. Secondary antibody was detected by using Pierce ECL Plus substrate (Thermo; 32132, 1:1 dilution) and detected by CCD camera, and specific band intensities were digitally quantified. Antibodies can be found in Table 1.

Real-Time PCR. Total RNA was isolated from individual corpus lutea from P8.5 ovaries from wild-type ($n = 7$), Becn1(fl/fl) cKO ($n = 7$), and Becn1(fl/Δ) cKO ($n = 6$) females. RNA was extracted from snap frozen tissue by using TRIzol reagent as per manufacturer's protocol for high proteoglycan samples (Life Technologies). Total RNA was subjected to DNase 1 treatment (Invitrogen) and then cleaned up on RNeasy spin columns (Qiagen). Total RNA was quantified by Nanodrop and analyzed by a 2100 Bioanalyzer (Agilent). Only RNA with a RNA Integrity Number (RIN) greater than 5 was used for cDNA synthesis. Total RNA (500 ng) was used for first-strand synthesis to create cDNA (Superscript III Reverse Transcriptase kit; Invitrogen). Detection of specific genes was performed on samples in triplicate by using SYBR Green PCR and quantified by the ΔΔCt method using primers shown in Table 2.

Electron and Light Microscopy. Ovaries were collected and used for routine preparation of transmission electron microscopy under supervision from the University of Kentucky Imaging Facility. Briefly, individual CL were dissected from ovaries, washed in ice-cold PBS, diced into ∼1 mm^3 cubes while in a droplet of freshly prepared 4% (wt/vol) paraformaldehyde/3.5% (vol/vol) glutaraldehyde in 0.1 M cacodylate buffer (PFA/GLA), and fixed by immersion in PFA/GLA for 2 h at 4 °C. After the first fixation, tissue pieces were washed four times with 8% (wt/vol) sucrose before postfixing with 1% OsO_4 for 1.5 h at 4 °C. After dehydration through a graded series of ethanol into propylene oxide, tissue pieces were infiltrated and embedded with Eponate 12 (PELCO). Embedded tissue pieces were sectioned to approximately 70 nm using a Reichert Ultracut E. Sections were then mounted on copper grids, stained with uranyl acetate followed by lead citrate, and observed by transmission electron microscopy (Philips Tecnai Biotwin 12). For light microscopy, an Olympus IX-71 microscope equipped with a DP72 CCD camera (Olympus) was used. Images were all similarly edited in Adobe Photoshop to subtract background.

Table 1. List of antibodies used

Primary/secondary antibodies	Species raised in	Manufacturer (Product no.)	Dilution used	Application (size in kDa)
Antigen				
Actin	Rabbit	Sigma (A2066)	1:10,000	WB (~46)
BECN1	Rabbit	Santa Cruz (sc-11427)	1:2,000	WB (~60)
GFP	Chicken	Aves Labs (GFP-1020)	1:500	IF
LC3	Rabbit	MBL (PM036)	1:2,000	WB (~14 and 16)
SQSTM1	Rabbit	Enzo (PW9860)	1:2,000	WB (~62)
StAR	Rabbit	Buck Hales, SIU	1:10,000	WB (~35)
Secondary antibodies				
Chicken IgY (H&L)	Goat	Invitrogen (A-11039)	1:500	IF
Rabbit IgG (H&L)	Donkey	Rockland (611-703-127)	1:10,000	WB

IF, immunofluorescence; SIU, Southern Illinois University; WB, Western blot.

Statistics. All statistics were performed in SigmaPlot 12 after consultation with the Applied Statistics Laboratory at the University of Kentucky. A two-way ANOVA was used with Holm–Sidak post hoc testing between groups for comparisons with two variables. For all other comparisons, the statistical test used is indicated in the text.

Results

Disruption of Becn1 in Mouse Luteal Cells. To analyze the role of autophagy in the CL, mice with conditional knockout (cKO) alleles for *Becn1* in luteal cells were generated by mating *Becn1*$^{fl/fl}$ with Tg(CYP19A1-cre)1Jri (*Cyp19-iCre*) mice (12, 19). Expression of *Cyp19-iCre* is restricted to granulosa cells of primary and secondary follicles that terminally differentiate into both large and small luteal cells after ovulation in rodents (24). Two experimental strains were generated: (*i*) *Cyp19-iCre*; *Becn1*$^{fl/fl}$ (Becn1(fl/fl) cKO) and (*ii*) *Cyp19-iCre*; *Becn1*$^{fl/\Delta}$ (Becn1(fl/Δ) cKO) (Fig. 1*A*). The siblings of the experimental strains that did not carry Cre were termed wild type and used as controls. Mice were born at the expected Mendelian ratios, and both males and females were otherwise healthy. To determine the extent of knockout, we performed Western blot analysis for BECN1 from granulosa cells of PMSG-primed females. BECN1 protein levels were decreased up to 75% in Becn1 (fl/fl) cKO, with a progressive reduction in the Becn1(fl/Δ) cKO, compared with Becn1(fl/Δ) controls (Fig. 1 *C* and *D*). This efficiency could be attributed to cell contamination, but more likely is due to the mosaicism of Cre-mediated gene recombination in Cre drivers. The turnover of the protein sequestosome 1 (SQSTM1), also known as p62, is used to monitor autophagy, and its accumulation

Table 2. Real-time PCR primers

Target	NCBI accession no.	Fwd and Rev Primer (5′-3′)	Amplicon size, bp
Lipe	NM_010719	CGC TGG AGG AGT GTT TTT TTG	66
		CAG TTG AAC CAA GCA GGT CAC A	
Hmgcr	NM_008255	TGT TCA CCG GCA ACA ACA AG	72
		TGC TCA GCA CGT CCT CTT CA	
Insig1	NM_153526	CGG CAG CGG CTG TTG	58
		GGT TCT CCC AGG TGA CTG TCA	
Star	NM_011485	CCG GAG CAG AGT GGT GTC A	65
		GCC AGT GGA TGA AGC ACC AT	
Cyp11a1	NM_019779	CCA GTG TCC CCA TGC TCA AC	73
		GCA TGG TCC TTC CAG GTC TTA G	
Hsd3b1	NM_008293	CCA GGC AGA CCA TCC TAG ATG	78
		TGG CAC ACT GGC TTG GAT AC	
Akr1c18	NM_134066	TGA TTG CCC TTC GCT ACC A	75
		TCT CTG ATT CTC TCC TCA TTG AAA CTC	
Lhcgr	NM_013582	GAC GCT AAT CTC GCT GGA GTT	152
		GTA GGA TGA CGT GGC GAT GA	
Prlr (long)	NM_011169	GCG TTC TTT GCA AGA AGT GCT	243
		CCA GGT GGT GAC TGT CCA TT	
Prlr (short)	NM_001253781	GGC TCT GAT AGA GCT CCC TG	156
		GCA ATA GAT CAG AGG CTC CCT TC	
Becn1	NM_019584	TTT TCT GGA CTG TGT GCA GC	171
		GCT TTT GTC CAC TGC TCC TC	
Atg7	NM_001253717	ATG CCA GGA CAC CCT GTG AAC TTC	349
		ACA TCA TTG CAG AAG TAG CAG CCA	
Pecam1	NM_008816	CCA AGG CCA AAC AGA	300
		AAG GGA GCC TTC CGT TCT	
Acat1	NM_144784	TGG GCG CAG GTT TAC CTA TT	63
		TTC CTG AAG CAC AAA CCT TGT TT	
Vegfa	NM_001025250	CAT CTT CCA GGA GTA CCC CGA	81
		CAC TCC AGG GCT TCA TCG TT	

Cyp11a1, cytochrome P450, family 11, subfamily A, polypeptide 1; Lhcgr, luteinizing hormone/choriogonadotropin receptor; Pecam1, platelet/endothelial cell adhesion molecule 1; Vegfa, vascular endothelial growth factor A.

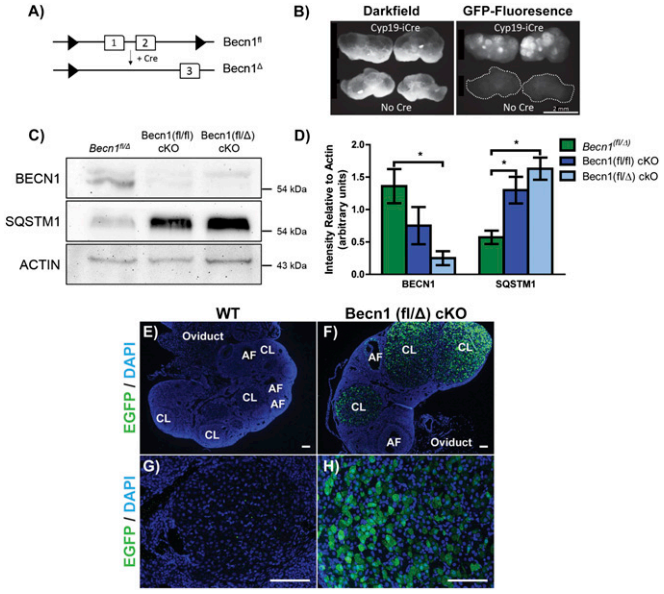

Fig. 1. Cyp19-iCre leads to recombination in the CL. (*A*) Genetic strategy to conditionally knock out Becn1. Numbered boxes correspond to exons with dashed boxes representing engineered insertions and triangles represent LoxP sites. (*B*) Ovaries from P8.5 CAG-CAT-EGFP females on both control and Cyp19-iCre backgrounds represented in darkfield and GFP-fluorescence with control ovaries outlined. (*C*) Representative immunoblots from granulosa cells 48 h after PMSG injection. (*D*) Quantified band intensity relative to Actin for BECN1 and SQSTM1, $n = 4$ for each genotype. Data represents mean with SEM. (*E–H*) Representative images showing immunofluoresence for EGFP, indicating Cre recombination, costained with DAPI on tissue sections from P8.5 ovaries. Low magnification was performed to see entire ovary (*E* and *F*). AF, antral follicle. High magnification of CL was to demonstrate recombination in luteal cells. (Scale bars: 100 μm.)

indicates an inhibition of autophagy (25, 26). As expected, *Becn1* deletion resulted in an almost threefold increase in SQSTM1 in the granulosa cells isolated from the cKO strains (Fig. 1*D*). Because the *Cyp19-iCre* mouse has shown variable Cre expression in follicles of naturally cycling animals (27, 28), we confirmed the extent of recombination in the Becn1(fl/Δ) cKO by crossing them onto a *CAG-CAT-EGFP* Cre-reporter background (22). Epifluorescent examination of ovaries from P8.5 indicated prominent GFP expression in the CLs of *CAG-CAT-EGFP*$^{+}$*; Cyp19-iCre; Becn1*$^{fl/\Delta}$ but not in *CAG-CAT-EGFP*$^{+}$*; Becn1*$^{fl/\Delta}$ in both large and small luteal cells (Fig. 1 *E–H*). GFP immunofluorescence on P8.5 tissue sections supports that recombination was robust throughout the CLs of Becn1(fl/Δ) cKO females (Fig. 1*H*). No recombination was detected in mammary glands, uterus, or placenta, which is supported by previous reports using the *Cyp19-iCre* mouse (19, 29).

To confirm luteal-specific gene deletion during pregnancy, Western blot analyses for BECN1 and SQSTM1 were performed on CLs isolated from P8.5 ovaries and normalized to ACTIN (Fig. 2 *A* and *B*). Both *Becn1* cKO strains had an approximate 50% reduction in BECN1 compared with controls. This result is expected because luteal cells comprise only ∼40% of the total cell population of the CL, and because other cell types present in the CL, such as pericytes, endothelial cells, and lymphocytes, also express BECN1 (30–33). Both *Becn1* cKO strains had a nearly fivefold increase in total SQSTM1 protein compared with control. Microtubule-associated protein 1B light chain 3 (LC3) is a protein that incorporates into the expanding autophagosome membrane. During expansion, the cytoplasmic form (LC3-I, ∼16 kDa) is processed to the membrane form (LC3-II, ∼14 kDa), which allows for an estimate of autophagosome quantity and autophagic flux by Western blot (34). LC3-I was increased almost threefold in both *Becn1* cKOs compared with controls. No LC3-II was detected in any CL sample, suggesting that LC3-II does not accumulate. Taken together, the accumulation of SQSTM1 and LC3-I indicate that autophagosome formation is impaired in Becn1(fl/fl) cKO and Becn1(fl/Δ) cKO corpora lutea. To determine that luteal cell differentiation had occurred, steroidogenic acute regulatory protein (StAR) was assayed by Western blot. StAR regulates the rate-limited step in steroidogenesis by transporting cholesterol from the outer to inner mitochondrial membrane (35). A trend for lower StAR protein was found in both *Becn1* cKOs compared with WT ($P < 0.07$), which suggested that StAR abundance may be affected by gene ablation.

Becn1 Is Necessary To Maintain Pregnancy. The number of implanted fetuses at P8.5 and ovarian size were equal for all strains, implying that ovulation, fertilization, and implantation are not affected by *Becn1* ablation (Fig. 2 *C* and *D*). To examine pregnancy success, 8- to 26-wk-old female mice were mated with wild-type male mice of proven fertility. All strains achieved pregnancy at similar rates in terms of percent bred and litter sizes when measured at P5.5; however, Becn1(fl/fl) cKO and Becn1(fl/Δ) cKO mice did not maintain their pregnancies and showed early parturition and abortion phenotypes, respectively. Becn1(fl/fl) cKO had a 10% reduced gestation length equal to 17.08 ± 0.25 d compared with control mice at P18.95 ± 0.12 d ($P < 0.001$, Dunn's multiple

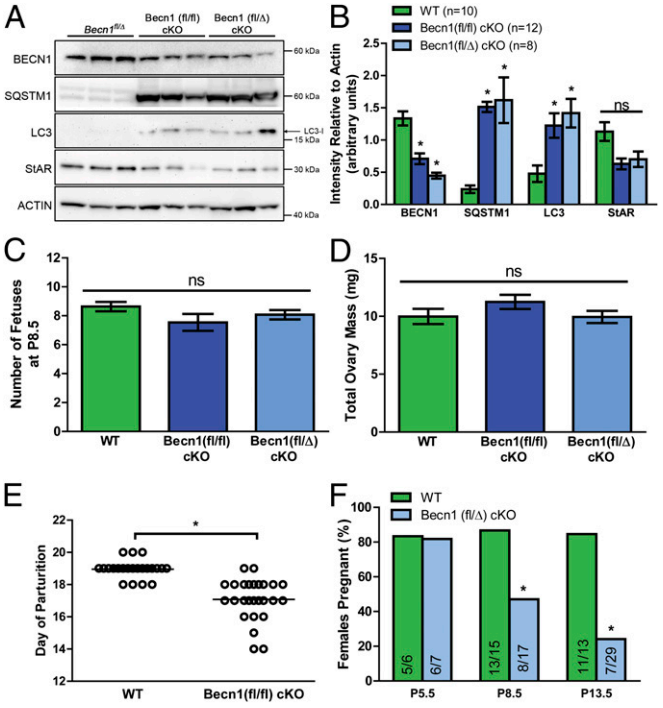

Fig. 2. *Becn1* is required to maintain pregnancy. (*A* and *B*) Immunoblots for P8.5 corpora lutea (*A*) from pregnant females and relative quantification (*B*). *$P < 0.05$ for Holm–Sidak post hoc test versus WT. **$P < 0.001$ for Dunn's multiple comparison test versus WT. *P* value for the StAR immunoblot was <0.07 and not significant as determined by ANOVA. (*C* and *D*) Number of implanted fetuses observed (*C*) and wet mass of both ovaries on P8.5 for individual strains (*D*). Data represent mean with SEM. (*E*) Histogram representing the day of parturition observed for WT ($n = 22$) and Becn1 (fl/fl) cKO ($n = 26$) females. Each data point represents a single pregnancy; bar is mean, *$P < 0.01$ for Dunn's multiple comparison test. (*F*) Percent of Becn1 (fl/Δ) cKO females that are pregnant on the designated day after mating. Observed number of pregnant females out of total females mated is indicated vertically inside each bar. *$P < 0.05$ for Fisher's exact test between the two genotypes.

comparison test, data represents mean ± SEM) (Fig. 2*E*). Litters born to Becn1 cKO mothers before P18.5 did not survive. Becn1 (fl/Δ) cKO mothers had a more pronounced phenotype and never gave birth to litters, despite females being visibly pregnant at P10.5 ($n = 28$ pregnancies). Reproductive tracts were collected at P5.5, P8.5, and P13.5 to determine when the implanted fetuses were lost. At P5.5, control and Becn1(fl/Δ) cKO females had the same pregnancy rate ($P = 1.00$, Fisher's exact test) (Fig. 2*F*). However, by P8.5, 46% fewer Becn1(fl/Δ) cKO females were pregnant compared with their control siblings ($P = 0.03$, Fisher's exact test). At P13.5, there were only 28% of Becn1(fl/Δ) cKO females pregnant compared with controls ($P < 0.001$, Fisher's exact test). Thus, Becn1(fl/Δ) cKO mice continuously lose their litters throughout pregnancy after implantation and Becn1(fl/fl) cKO mice give birth an average of 2 d earlier than controls.

Becn1 Is Required for Progesterone Synthesis During Midpregnancy. To quantify progesterone levels, plasma was collected every other day from control and Becn1(fl/fl) cKO females beginning at P1.5 until parturition. Because 46% of Becn1(fl/Δ) cKOs lost their pregnancy by P8.5, plasma was collected every day from P1.5 to P7.5 to quantify progesterone. Progesterone production in both the Becn1(fl/fl) cKO and Becn1(fl/Δ) cKO were equivalent to controls through P7.5 (Fig. 3*A*). Becn1(fl/fl) cKO progesterone levels peak at P9.5 with a mean of 51.0 ng/mL. After P11.5, Becn1 (fl/fl) cKO mice had a drop in progesterone, whereas in control mice, levels increased at P13.5 and then remained elevated until P17.5. Thus, *Becn1* is required for increased levels of serum progesterone that occur during mid to late pregnancy, but is not required during early pregnancy.

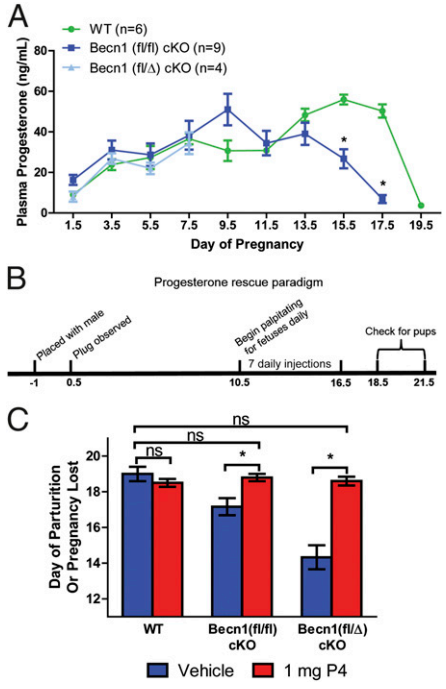

Fig. 3. *Becn1* cKO early parturition is progesterone-dependent. (*A*) Progesterone quantified from plasma every other day throughout pregnancy for WT, Becn1 (fl/fl) cKO, and Becn1 (fl/Δ) cKO. Data represents mean with SEM. *$P < 0.05$ for Holm–Sidak post hoc test versus WT for that day. (*B*) Diagram depicting dosing paradigm for exogenous progesterone administration. (*C*) Day of parturition for females that were given sesame oil (vehicle) or 1 mg of progesterone daily ($n \geq 3$ for each group). Data represents mean with SEM. *$P < 0.001$ for Holm–Sidak post hoc test for interaction indicated. ns, not significant.

In an attempt to rescue litters and test whether the loss of progesterone was the cause of loss of litters, exogenous progesterone administration was given to control, Becn1(fl/fl) cKO, and Becn1(fl/Δ) cKO dams starting on P10.5 until P16.5 in an attempt to rescue gestation length and pregnancy (Fig. 3*B*). Vehicle-treated dams for all three groups gave birth similar to previous results from nontreated animals (Fig. 3*C*). Control mice ($n = 4$) had their litters on P19.0 ± 0.41; Becn1(fl/fl) cKOs ($n = 6$) gave birth on P17.2 ± 0.48; Becn1(fl/Δ) cKO ($n = 3$) lost their pregnancy as determined by palpitation by P14.3 ± 0.67 (data represents mean ± SEM) (Fig. 3*C*), consistent with our previous observations (Fig. 2*F*). Exogenous progesterone had no effect on control mice ($n = 6$), because they gave birth on P18.5 ± 0.22 ($P = 0.8$, Holm–Sidak post hoc test). However, progesterone-treated Becn1(fl/fl) cKO ($n = 5$) had an extended gestation length equivalent to controls giving birth on P18.8 ± 0.2 ($P < 0.01$ vs. vehicle, $P = 0.7$ vs. control, Holm–Sidak post hoc test) (Fig. 3*C*). Moreover, progesterone-treated Becn1(fl/Δ) cKO mice ($n = 5$) had increased gestation periods equivalent to controls, giving birth to live litters on P18.6 ± 0.25 ($P < 0.001$ vs. vehicle, $P = 0.8$ vs. control, Holm–Sidak post hoc test) (Fig. 3*C*). Therefore, exogenous progesterone corrected for the reduced gestation and abortion resulting from *Becn1* ablation.

To test whether the hypothalamus-pituitary-gonadal (HPG) axis was affected by *Becn1* deletion in luteal cells, serum at diestrus, P13.5, and P16.5 was collected to quantify estradiol, FSH, and LH. No differences between WT and Becn1(fl/fl) cKO were detected at diestrus (Fig. 4 *B*–*E*). Estradiol at P13.5 was increased in Becn1(fl/fl) cKO compared with WT ($P < 0.05$, Holm–Sidak post hoc test), but by P16.5, no difference was detected ($P = 0.6$, Holm–Sidak post hoc test) (Fig. 4*C*). FSH concentrations were inverse to estradiol with reduced concentration in Becn1(fl/fl) cKO at P13.5 and no difference at P16.5 (Fig. 4*D*). No difference was detected in LH at P13.5 or P16.5 (Fig. 4*E*). In addition, no difference in estrous cyclicity was found between WT and Becn1(fl/fl) cKO (Fig. 4*A*). This data indicates that the HPG axis is not affected by *Becn1* ablation and suggests that progesterone reduction is not due to systemic effects. The issue may be due to a lack of placental lactogen to stimulate progesterone during the window P11.5–13.5.

Becn1 Is Required for Lipid Droplet Formation Within Luteal Cells. The reduction in circulating progesterone could result from reduced progesterone synthesis within luteal cells or an up-regulation of progesterone metabolizing enzymes, such as 20α-HSD (36). Free cholesterol, the substrate of progesterone synthesis, is created through hydrolysis of intracellular cholesteryl ester that is stored within lipid droplets, a common characteristic of luteal cells. To determine whether lipid stores were present in Becn1 (fl/Δ) cKO luteal cells, P8.5 and P13.5 ovary sections were stained for neutral lipids by using Oil Red O. All ovaries, regardless of genotype, showed expected staining in the ovarian medulla and in the theca at both P8.5 and P13.5 (Fig. 5 *A*, *B*, *E*, and *F*). At low magnification, staining was evident in the CLs from control females at both P8.5 and P13.5, with a qualitative increase as gestation time increases (Fig. 5 *C* and *G*). However, the CLs of Becn1(fl/Δ) cKOs have reduced staining compared with controls at both time points, suggesting a reduction in neutral lipid storage (Fig. 5 *B* and *F*). At higher magnification, numerous red staining puncta were apparent in luteal cells from control ovaries indicating the presence of lipid droplets (Fig. 5 *C* and *G*). Becn1(fl/Δ) cKO luteal cells were rarely positive for staining (Fig. 5 *D* and *H*, arrowheads), suggesting a failure in neutral lipid storage.

Electron micrographs show that Becn1(fl/Δ) cKO luteal cells exhibited an accumulation of autophagosomes containing what appears to be numerous organelles and cytoplasmic contents, not present in control luteal cells (Fig. 6*F*). There were also fewer lipid droplets, extensive cytoplasmic vacuolation, and the absence of multivesicular bodies in Becn1(fl/Δ) cKO luteal cells compared

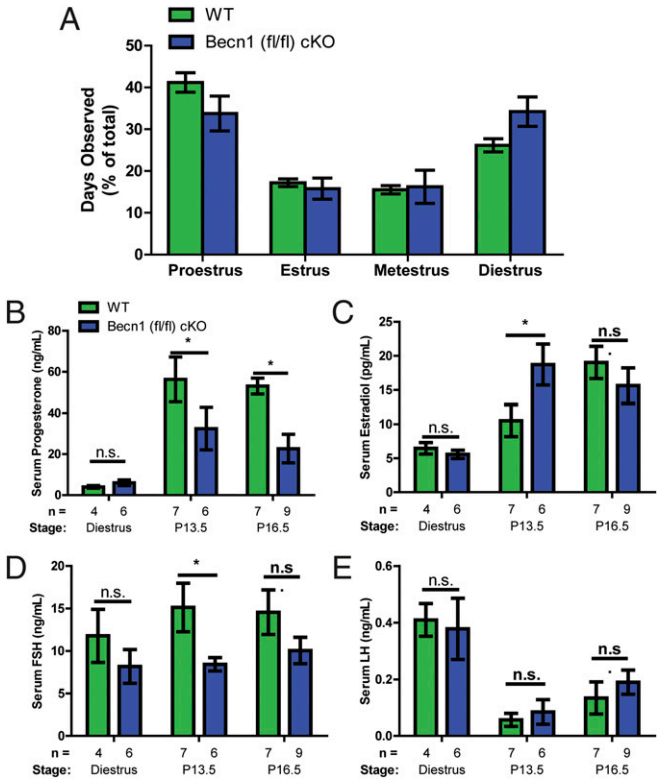

Fig. 4. Becn1 (fl/fl) cKO hormone profile and estrus cyclicity are normal. (*A*) Percent of time that each estrus stage was observed for WT ($n = 20$) and Becn1 (fl/fl) cKO ($n = 15$) over 21 d. Data represents mean with SEM. *P* value equals 0.09 for two-way ANOVA for genotype x stage interaction. (*B–E*) Reproductive hormones progesterone (*B*), estradiol (*C*), follicle-stimulating hormone (*D*), and luteinizing hormone (*E*) quantified from serum collected during euthanasia at the specified times. For all charts, data represents mean with SE of mean. $*P < 0.05$ for Holm–Sidak post hoc test versus WT. ns, not significant.

with control cells (Fig. 6 *A*, *B*, *D*, and *E*). Endoplasmic reticulum (ER) membrane expansion was distinct in WT luteal cells observed as numerous small circular single membrane inclusions, or cross-sections of the endoplasmic reticulum tubules (Fig. 6 *C* and *E*). Qualitatively, reduced ER expansion as evidence of the presence of whorls in Becn1(fl/Δ) cKO luteal cells suggested that ER swelling was not occurring and that steroidogenesis was reduced (Fig. 6*D*). In addition to ER swelling, the presence of enlarged mitochondria is typically found in steroid-producing cells (37). Mitochondria in the control luteal cells were lightly staining, round, and swollen, which indicated that steroid production was occurring (Fig. 6*A*). In contrast, mitochondria in Becn1(fl/Δ) cKO luteal cells were smaller and darkly staining, which suggested a defect in steroidogenesis (Fig. 6*B*).

***Becn1* Ablation Causes Down-Regulation of Genes in the Progesterone Feedback Network.** Because progesterone production depends on several genes that can be grouped into the "cholesterol accumulation," "progesterone synthesis," and "signal regulation" transcription networks, we quantified the transcriptional networks devoted to progesterone production in the Becn1 cKO models. Total mRNA from P8.5 CL were analyzed because this time point preceded the drop in progesterone production and reflected a lipid store reduction in the Becn1(fl/Δ) cKO. Differences were detected in the "cholesterol synthesis" genes of Becn1(fl/fl) cKOs compared with WT mice (Fig. 7). A significant reduction was found for *Acat1* ($P < 0.5$) and a trend in reduced expression for *Hmgcr* and *Insig1* in the Becn1(fl/fl) cKO group. However, there were no differences in any of the progesterone synthesis genes of Becn1(fl/fl) cKO or Becn1(fl/Δ) cKO mice compared with WT mice. In the "feedback" network gene group, there was a trend for reduced levels of *Lhgcr* [significant for the Becn1(fl/fl) cKO group] and the long-form of *Prlr* (*Prlr-L*) in Becn1(fl/fl) and Becn1(fl/Δ) cKO mice compared with WT. A reduction in the short form of the prolactin receptor (*Prlr-S*) in these cKO models suggests that *Becn1* positively regulates the expression of the regulatory network genes. *Becn1* ablation was confirmed in the cKO model by showing a reduction in the transcripts for *Becn1*. No up-regulation in autophagy was found as determined by similar expression of *Atg7* in all groups. Finally, examination of luteal vasculature through expression of the endothelial marker gene *Pecam* was similar across genotypes, indicative of similar vascularization. In contrast, *Vegfa* factor produced by luteal cells that can impact endothelial proliferation as well as function, i.e., vascular permeability, was decreased in the Becn1(fl/fl) cKO group compared with wild type.

Becn1 Is Required for Endosome and LC3-Positive Vesicle Clearance. To determine the level of autophagic flux, *GFP-LC3#53* (GFP-LC3) mice that express GFP-LC3 under a CAG promoter were used to track autophagosomes as GFP puncta (21, 38). *GFP-LC3*$^{+}$;

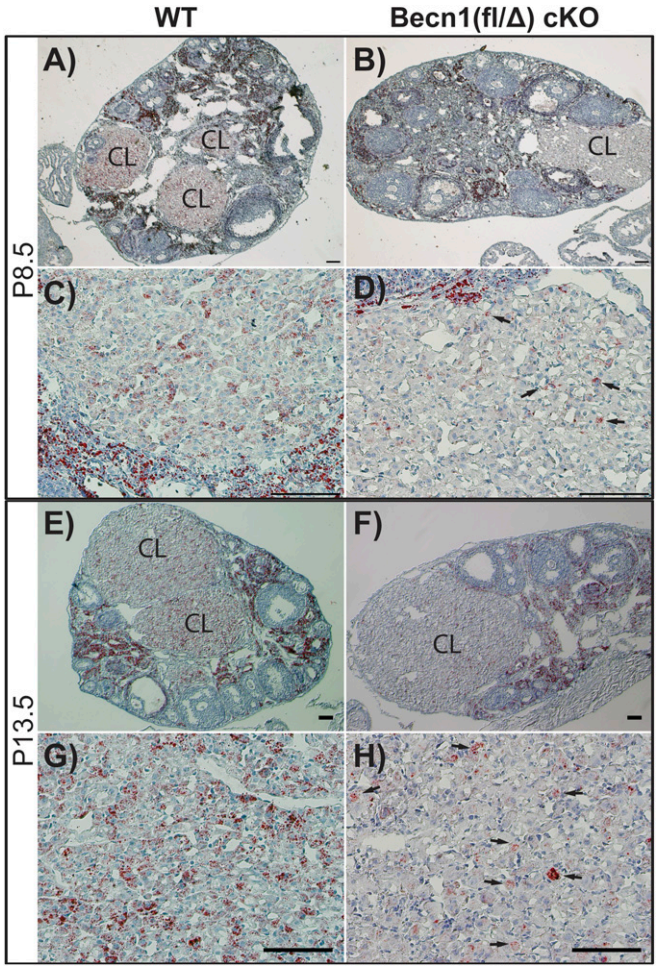

Fig. 5. *Becn1* promotes neutral lipid stores in luteal cells. Representative images of frozen tissue sections stained with Oil Red O (red) and counterstained with hematoxylin (blue) at P8.5 (*A–D*) and P13.5 (*E–H*). Low magnification indicates staining in medulla, theca, and corpus lutea (*A*, *B*, *E*, and *F*). Higher magnification of CL highlights luteal cell staining (*C–E* and *H*). Oil Red O stains neutral lipids, mainly observed as lipid droplets (arrows). (Scale bars: 100 μm.)

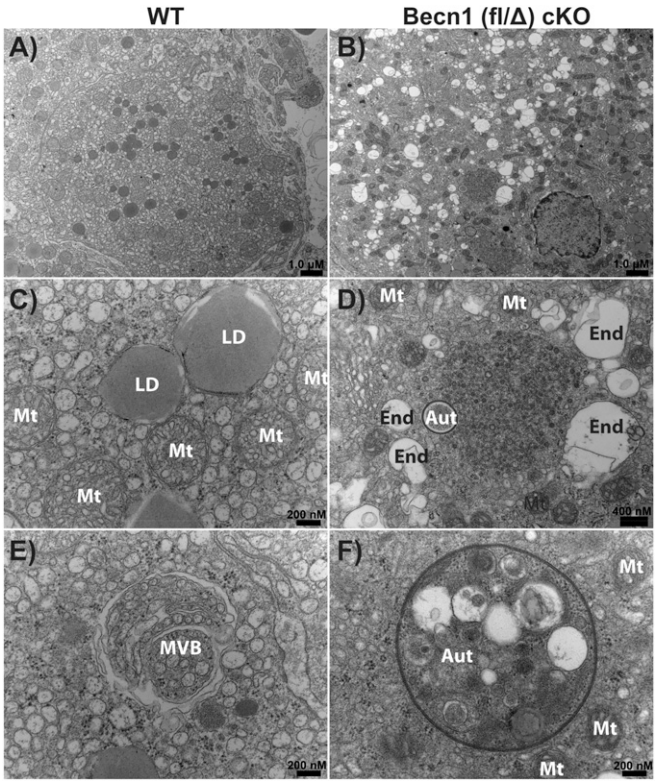

Fig. 6. *Becn1* is necessary for the clearance of autophagosomes and endosomes. Representative images from transmission electron microscopy of P13.5 large luteal cells from WT (*A*, *C*, and *E*) and Becn1 (fl/Δ) cKO (*B*, *D*, and *F*). An entire cell ultrastructure where lipid droplets mitochondria and nuclei are seen (*A* and *B*). High magnification images indicate mitochondria (Mt), lipid droplets (LD), multivesicular bodies (MVB), endosome (End), and autophagosomes (Aut) (*C*–*F*). Scale is indicated on the lower right corner of each image.

Becn1(fl/Δ) cKO and *GFP-LC3*$^{+}$; control ovaries were collected at P8.5 and P13.5 for epifluorescence on tissue sections. Qualitatively, very few GFP puncta were observed at either time point in WT luteal cells (Fig. 8 *A*, *C*, *E*, and *G*). Granulosa cells and oocytes appeared to contain more GFP puncta compared with luteal cells, with no observable difference from P8.5 and P13.5 (Fig. 8 *A* and *E*), implying high autophagic flux in control luteal cells. However, luteal cells from Becn1(fl/Δ) cKO ovaries had multiple large GFP puncta, sometimes comprising the entirety of the cell (Fig. 8 *B*, *D*, *F*, and *H*).

Discussion

This study has demonstrated that *Becn1* is essential in female reproduction for proper functioning of the CL during pregnancy. Beyond the reproductive phenotype, there are broader implications that impact different facets of cell biology in which autophagy or autophagy-related proteins play a part, namely lipid metabolism and steroidogenesis. Autophagy and the mobilization of lipids from lipid droplets are intimately linked in a catabolic process termed lipophagy, where autophagosomes deliver small inclusions of lipid droplets to lysosomes (39). Utilization of lipid stores, especially cholesterol, is important for steroidogenic cells to produce mineralocorticoids, glucocorticoids, estrogens, androgens, and progesterone. These steroid hormones have a systemic effect on sexual development and immunity, inflammation, and metabolism. Although autophagy is already well known to be important in normal development and disease states (40), there remain gaps in the underlying biochemical basis for these links. Understanding how *Becn1* and autophagy integrate lipid metabolism and steroid production would help to bridge these gaps.

Autophagy is also suggested to positively regulate the growth and accumulation of lipid droplets in some tissues, including in adipose tissue of obese and diabetic individuals (41). However, the role of *Becn1* in lipid droplet regulation has only been recently explored. Knockout of the *Saccharomyces cerevisiae Atg6* homolog inhibits the degradation of lipid droplet-specific proteins Faa4-GFP and Egr6-GFP by the vacuole (42), suggesting that *Atg6* participates in lipid droplet degradation. Additional knockdown studies support the idea of a conserved function for *Becn1* to positively affect lipid droplet formation and growth. Knockdown of the *Drosophila Atg6* reduces the size of lipid droplets in the larval fat body (43). *Caenorhabditis elegans* with a mutated Bec-1 have reduced numbers of lipid droplets throughout development regardless of diet (44). Similarly, knockdown of *Becn1* in cultured 3T3-L1–induced adipocytes reduces lipid storage as detected by neutral lipid staining (45). In this study, we show that knockout of *Becn1* in mouse luteal cells reduces lipid storage, which would lead to a reduction in progesterone synthesis, supporting that BECN1 is a component in lipid droplet maintenance. Cholesterol biosynthesis takes place within the ER by using acetyl-CoA as a substrate and is regulated by the rate-limiting enzyme 3-hydroxy-3-methylglutaryl CoA (HMGCoA) reductase (HMGCR) (46). To facilitate storage or transport, cholesterol is dehydrated to cholesteryl ester by acyl-CoA:cholesterol acetyltransferase 1 (ACAT1) in the ER (47). The amount of free cholesterol is regulated through a negative feedback loop in the endoplasmic reticulum by insulin-induced gene 1 (INSIG1). Under high sterol concentrations, INSIG1 is expressed to negatively regulate HMGCR transcription and directly increase the degradation of HMGCR (48). The reduction of *Acat1* in our model would indicate a reduction in cholesterol synthesis. Whether lipid droplet formation and cholesterol synthesis is a direct or indirect function of BECN1 needs to be addressed in future experiments.

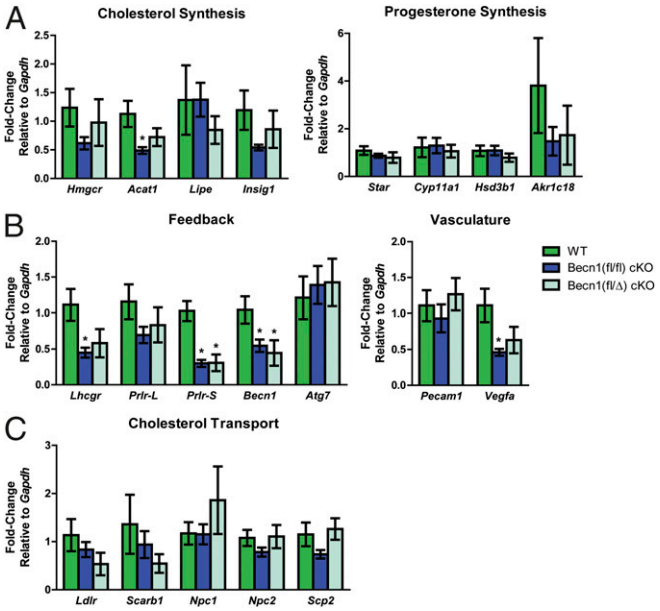

Fig. 7. Effects of the *Becn1* cKO on the progesterone gene network. mRNA expression relative to wild-type and normalized to β-*actin* and *Gapdh* for genes for progesterone synthesis (*A*), cholesterol transport and synthesis (*B*), and luteal cell signaling (*C*) in isolated individual corpus lutea from P8.5 ovaries. Data represents mean with SEM for $n \geq 4$ for each group. *$P < 0.05$ for Holm–Sidak post hoc test versus WT individually for each gene.

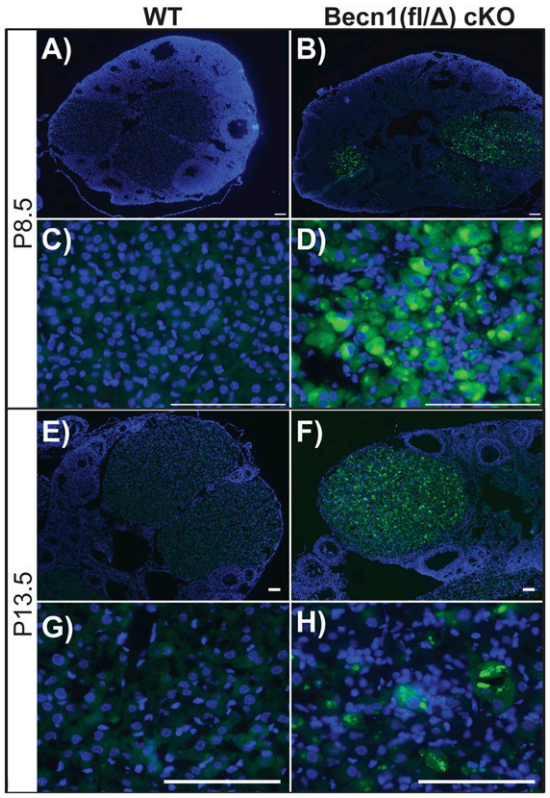

Fig. 8. *Becn1* is necessary for the clearance of GFP-positive vesicles. Representative images of frozen tissue sections directly viewed for GFP-LC3. Low magnification (*A*, *B*, *E*, and *F*) shows that only CLs of Becn1 (fl/Δ) cKO have intense GFP. GFP-LC3 puncta are present in Becn1 (fl/Δ) cKO (*D* and *H*) but not in WT luteal cells (*C* and *G*). (Scale bars: 100 μm.)

In addition to regulation of intracellular lipid stores, BECN1 may have a role in the trafficking of extracellular cholesterol. Extracellular cholesterol is required for acute steroidogenesis, and circulating HDLs and LDLs provide the predominant source of cholesterol to luteal cells through receptor-mediated endocytosis. After endocytosis, endosomes mature and fuse with lysosomes where the cholesterol esters are hydrolyzed and transported out of the lysosome. LDL receptors are recycled back to the plasma membrane to facilitate further transport approximately every 10 min to maintain cholesterol influx (49). Receptor-mediated endocytosis is primarily used to transport LDL particles, but HDL has been observed in endosomes (50). Substantial evidence demonstrates a role for BECN1 in endosome maturation. BECN1 forms a conserved complex with VPS15, VPS34, UVRAG, and Bif-1 that is necessary for autophagosome and endosome to lysosome fusion in *Drosophila*, *C. elegans*, mouse, and human cells (51–54). Furthermore, epithelial growth factor receptor undergoes endosome-mediated membrane recycling that requires the BECN1 complex (51, 55, 56). Epifluorescence and electron microscopy of Becn1 (fl/Δ) cKO luteal cells indicate an increased number of large autophagosomes and a dramatic increase in the number of endosomes. It is possible that these endosomes are sequestering lipoprotein receptors, such as LDL receptors, to dampen the transport of cholesterol into the cells. Thus, the cells cannot synthesize lipid droplets because of reduced lipid transport. It will be necessary to characterize lipoprotein transporters in these endosomes and to identify whether these vesicles are retrograde endosomes or secretory vesicles.

Autophagy has had a causal, functional link to both follicular atresia and CL regression; however, in vivo genetic-based validation studies have not been reported. Previous in vitro studies have linked autophagy and apoptosis in granulosa cells to follicular atresia (57, 58). Autophagosomes have been detected in granulosa cells of atretic follicles in several species including rat (59), ewe (60), bovine (61), characiform fish (62), goose (63), quail (64), and human (65). In addition, autophagic vacuoles were first reported in the regressing CL of humans and guinea pigs more than 40 y ago (66–69). Supporting a link between autophagy and steroidogenesis, pharmacological induction of the endocrine type of voltage-activated sodium channel promoted autophagosome and secondary lysosome formation while reducing progesterone levels in human granulosa cells (70). BECN1 has been immunolocalized to theca-lutein and granulosa-lutein regions in human ovaries after ovulation, and also has been speculated to regulate the life span of the CL (71). We find that *Becn1* and autophagy regulate the functional life span of the CL, because progesterone production is prematurely terminated during pregnancy. This is the first genetic approach, to our knowledge, to study the in vivo function of autophagy in the CL, and one of the first to use the *Cyp19-iCre* mouse to study CL gene function. This Cre model initially was used to conditionally ablate *Pten* in granulosa cells, which did not alter steroidogenesis but delayed luteolysis (19). The *Cyp19-iCre* model is highly cell-specific, although similar to most transgenic lines does not reach 100% efficiency because of mosaic expression. Although we could have contamination with other cell types during the isolation of granulosa cells from PMSG-primed follicles, the protein reduction we found in our study is comparable to that found after deletion of the floxed epidermal growth receptor gene by using the same Cre driver (27). Although the exact role of autophagy in granulosa/luteal cell function is not clear, autophagy is generally hypothesized to be a critical regulator of cell metabolism and homeostasis (72). With respect to other reproductive tissues, *Becn1* has been linked to testosterone production in mouse Leydig cells (73). This data nicely dovetails our findings and suggests that *Becn1* has a broader role in steroid production in other organs.

Prolactin (PRL) signaling provides an important positive feedback loop to maintain progesterone production during pregnancy. Upon cervical stimulation during coitus, PRL secreted from the anterior pituitary and, along with FSH and LH, form a luteogenic complex that signals through PRLR and LHCGR on the luteinizing granulosa cells to promote CL formation and progesterone synthesis. Two forms of PRLR are found in CLs, the short and long forms activate many kinases including Src kinase, phosphatidylinositol-3-kinase, mitogen-activated protein kinase, and Nek3-vav2-Rac1; however, only the long form of PRLR (PRLR-L) is shown to activate Jak2/Stat5 (74). These downstream signals indirectly and directly regulate gene expression of all components of the progesterone network, including PRLR and LHCGR. Although PRLR signaling initially depends on pituitary PRL during early pregnancy, there is a gradual shift toward a reliance on two placenta-derived homologs, placental-lactogen I and II (PL-I, PL-II). From P6 to P10, PL-I is produced and functionally complements the mother's pituitary PRL (75). On P9, PL-II begins to be secreted and remains high until parturition (76). By P11, the mother no longer secretes PRL, and PL-I and PL-II are solely responsible for signaling through PRLR-L. Our quantitative PCR (Q-PCR) data showed a down-regulation of the prolactin signaling network transcripts for *Prlr-S*. Consistent with our observation, mice that lacked *Prlr-S*, but expressed the *Prlr-L* form, exhibited reduced luteal function. These mice had an early CL regression, loss of progesterone production, and implantation failure due to alterations in angiogenesis and vascularization (77). The more aggressive phenotype (i.e., loss of angiogenesis and early CL regression) in the *Prlr-S*–deficient mice might be due to its complete loss, compared with a 75% knockdown in our model. Expression of both forms of the prolactin receptor is important in CL formation and maintenance. Transgenic mice only expressing the short form (PRLR-S) in luteal cells do not have proper CL formation or

function, and exhibit premature ovarian failure (78). Our model may not have altered angiogenesis in the CL, as shown by *Pecam* expression, but may have differences in vascular permeability as suggested by the reduction in *Vegfa* expression. A change in the function of the vasculature may suggest that luteal cells are not responding to PRL and LH to produce growth factors. It will be necessary to examine in the future whether these signaling pathways are attenuated in the model. Interestingly, there was not a reduction in the transcripts for progesterone biosynthesis proteins StAR and CYP11A1, although we did find a reduction in *Lhcgr* message. Although StAR ablation causes an increase in lipid droplet formation within adrenal and Leydig cells, there is no corresponding pathology found in the ovary in young mice (79). It is possible that BECN1 is involved in receptor recycling in the CL to attenuate cell signaling, as has been demonstrated in phagosome receptor recycling in human Alzheimer's disease brains (80).

Increasing numbers of couples in the United States actively seek treatment for infertility each year, impacting nearly 20% of couples. Research has focused on understanding both environmental and genetic causes leading to conception or pregnancy failure. The source of genetic problems can stem from male- or female-associated defects, or a combination of both. A functional consequence of our conditional knockout approach is the generation of a unique model for preterm birth. Preterm birth, a human-specific term defined as parturition at less than 37 wk of gestation and full term being 39 wk (81), occurs in an estimated 1 in 8 pregnancies and is the leading cause of neonatal deaths (82). There are relatively few mouse models that have demonstrated a preterm birth phenotype, and these mouse models include the following: lipopolysaccharide inflammatory response (83), acute alcohol exposure in late pregnancy (84), progesterone-receptor antagonism (85), *Stat5b* knockout mice (86, 87), inactivation of cannabinoid receptor CB1 (88), and *Trp53* deletion in progesterone receptor expressing cell linages (89). A unique distinction of our model is that the gestation length was rescued by exogenous progesterone administration, the only proven clinical treatment for women with a history of preterm birth (90–92). Progesterone production in humans is different in that the syncytiotrophoblast of the placenta is the progesterone producing cells after the first 8 wk of gestation (93). Despite this difference, a BECN1 deficiency could be a major contributor to preterm birth in humans. A recent study reported steady mRNA and protein expression of BECN1 in villous placental tissue collected from 7 wk of gestation to full-term birth (94). Studying the function of *Becn1* in human placenta would be an opportunity to characterize a novel pathway that could be affected during preterm birth. Our Q-PCR data revealed that steroidogenic enzyme expression is not reduced in our model; however, the biochemical pathway to progesterone will need to be further characterized. Thus, the luteal cell-specific deletion of *Becn1* offers an interesting model for future studies to help understand the regulation of preterm labor and gives insight to possible roles for *Becn1* in human pregnancy.

In summary, we have shown the importance of autophagy and *Becn1* on female reproduction, and have implicated lipid regulation and steroid production as being affected in the absence of *Becn1*. Future experiments should delve more deeply into the autophagy-dependent and autophagy-independent functions for BECN1 in this implicated process in the ovary. Elucidation of these functions will be important to understand how autophagy is intimately linked to development in other organs and cell types. Our findings may also have direct relevance in the context of how BECN1, already associated with many human diseases, is related to normal human reproduction and infertility.

ACKNOWLEDGMENTS. We thank Maggie Murphy for assistance with lipid staining, Wendy Katz for assistance with tissue embedding through support of the University of Kentucky Center of Research in Obesity and Cardiovascular Disease COBRE P20 GM103527-06, and Frontiers in Reproduction for expanding the knowledge of T.R.G. and the science underlying this project. This work was supported by Kentucky Science and Engineering Funds KSEF 2305-RDE-014 and, in part, by a Research Support Grant from the University of Kentucky Office of the Vice President for Research (to E.B.R.), a Gertrude Flora Ribble Fellowship (to T.R.G.), and National Institute of Child Health and Human Development Grant HD061580 (to L.K.C.).

1. Edinger AL, Thompson CB (2003) Defective autophagy leads to cancer. *Cancer Cell* 4(6):422–424.
2. Klionsky DJ, Emr SD (2000) Autophagy as a regulated pathway of cellular degradation. *Science* 290(5497):1717–1721.
3. Mehrpour M, Esclatine A, Beau I, Codogno P (2010) Overview of macroautophagy regulation in mammalian cells. *Cell Res* 20(7):748–762.
4. Nakatogawa H, Suzuki K, Kamada Y, Ohsumi Y (2009) Dynamics and diversity in autophagy mechanisms: Lessons from yeast. *Nat Rev Mol Cell Biol* 10(7):458–467.
5. Thumm M, et al. (1994) Isolation of autophagocytosis mutants of Saccharomyces cerevisiae. *FEBS Lett* 349(2):275–280.
6. Tsukada M, Ohsumi Y (1993) Isolation and characterization of autophagy-defective mutants of Saccharomyces cerevisiae. *FEBS Lett* 333(1-2):169–174.
7. Liang XH, et al. (1999) Induction of autophagy and inhibition of tumorigenesis by beclin 1. *Nature* 402(6762):672–676.
8. Qu X, et al. (2003) Promotion of tumorigenesis by heterozygous disruption of the beclin 1 autophagy gene. *J Clin Invest* 112(12):1809–1820.
9. Kihara A, Kabeya Y, Ohsumi Y, Yoshimori T (2001) Beclin-phosphatidylinositol 3-kinase complex functions at the trans-Golgi network. *EMBO Rep* 2(4):330–335.
10. Levine B, Kroemer G (2009) Autophagy in aging, disease and death: The true identity of a cell death impostor. *Cell Death Differ* 16(1):1–2.
11. Mizushima N, Levine B (2010) Autophagy in mammalian development and differentiation. *Nat Cell Biol* 12(9):823–830.
12. Gawriluk TR, et al. (2011) Autophagy is a cell survival program for female germ cells in the murine ovary. *Reproduction* 141(6):759–765.
13. Conneely OM, Mulac-Jericevic B, Arnett-Mansfield R (2007) Progesterone signaling in mammary gland development. *Ernst Schering Found Symp Proc* 1:45–54.
14. Conneely OM, Mulac-Jericevic B, DeMayo F, Lydon JP, O'Malley BW (2002) Reproductive functions of progesterone receptors. *Recent Prog Horm Res* 57:339–355.
15. Carr BR, MacDonald PC, Simpson ER (1982) The role of lipoproteins in the regulation of progesterone secretion by the human corpus luteum. *Fertil Steril* 38(3):303–311.
16. Miller WL, Bose HS (2011) Early steps in steroidogenesis: Intracellular cholesterol trafficking. *J Lipid Res* 52(12):2111–2135.
17. Singh R, et al. (2009) Autophagy regulates lipid metabolism. *Nature* 458(7242):1131–1135.
18. Zhang Y, et al. (2009) Adipose-specific deletion of autophagy-related gene 7 (atg7) in mice reveals a role in adipogenesis. *Proc Natl Acad Sci USA* 106(47):19860–19865.
19. Fan HY, Liu Z, Cahill N, Richards JS (2008) Targeted disruption of Pten in ovarian granulosa cells enhances ovulation and extends the life span of luteal cells. *Mol Endocrinol* 22(9):2128–2140.
20. Jamin SP, Arango NA, Mishina Y, Hanks MC, Behringer RR (2002) Requirement of Bmpr1a for Müllerian duct regression during male sexual development. *Nat Genet* 32(3):408–410.
21. Mizushima N, Yamamoto A, Matsui M, Yoshimori T, Ohsumi Y (2004) In vivo analysis of autophagy in response to nutrient starvation using transgenic mice expressing a fluorescent autophagosome marker. *Mol Biol Cell* 15(3):1101–1111.
22. Kawamoto S, et al. (2000) A novel reporter mouse strain that expresses enhanced green fluorescent protein upon Cre-mediated recombination. *FEBS Lett* 470(3):263–268.
23. Mann JS, Kindy MS, Edwards DR, Curry TE, Jr (1991) Hormonal regulation of matrix metalloproteinase inhibitors in rat granulosa cells and ovaries. *Endocrinology* 128(4):1825–1832.
24. Stocco C, Telleria C, Gibori G (2007) The molecular control of corpus luteum formation, function, and regression. *Endocr Rev* 28(1):117–149.
25. Bjørkøy G, et al. (2005) p62/SQSTM1 forms protein aggregates degraded by autophagy and has a protective effect on huntingtin-induced cell death. *J Cell Biol* 171(4):603–614.
26. Ichimura Y, Kominami E, Tanaka K, Komatsu M (2008) Selective turnover of p62/A170/SQSTM1 by autophagy. *Autophagy* 4(8):1063–1066.
27. Hsieh M, Thao K, Conti M (2011) Genetic dissection of epidermal growth factor receptor signaling during luteinizing hormone-induced oocyte maturation. *PLoS ONE* 6(6):e21574.
28. Bennett J, Wu YG, Gossen J, Zhou P, Stocco C (2012) Loss of GATA-6 and GATA-4 in granulosa cells blocks folliculogenesis, ovulation, and follicle stimulating hormone receptor expression leading to female infertility. *Endocrinology* 153(5):2474–2485.
29. Fan HY, et al. (2008) Selective expression of KrasG12D in granulosa cells of the mouse ovary causes defects in follicle development and ovulation. *Development* 135(12):2127–2137.
30. Lei ZM, Chegini N, Rao CV (1991) Quantitative cell composition of human and bovine corpora lutea from various reproductive states. *Biol Reprod* 44(6):1148–1156.
31. Fu D, et al. (2012) Mechanisms of modified LDL-induced pericyte loss and retinal injury in diabetic retinopathy. *Diabetologia* 55(11):3128–3140.
32. Nguyen TM, Subramanian IV, Kelekar A, Ramakrishnan S (2007) Kringle 5 of human plasminogen, an angiogenesis inhibitor, induces both autophagy and apoptotic death in endothelial cells. *Blood* 109(11):4793–4802.

33. Arsov I, et al. (2011) A role for autophagic protein beclin 1 early in lymphocyte development. *J Immunol* 186(4):2201–2209.
34. Kabeya Y, et al. (2000) LC3, a mammalian homologue of yeast Apg8p, is localized in autophagosome membranes after processing. *EMBO J* 19(21):5720–5728.
35. Black SM, Harikrishna JA, Szklarz GD, Miller WL (1994) The mitochondrial environment is required for activity of the cholesterol side-chain cleavage enzyme, cytochrome P450scc. *Proc Natl Acad Sci USA* 91(15):7247–7251.
36. Albarracin CT, Parmer TG, Duan WR, Nelson SE, Gibori G (1994) Identification of a major prolactin-regulated protein as 20 alpha-hydroxysteroid dehydrogenase: Coordinate regulation of its activity, protein content, and messenger ribonucleic acid expression. *Endocrinology* 134(6):2453–2460.
37. Amsterdam A, Knecht M, Catt KJ (1981) Hormonal regulation of cytodifferentiation and intercellular communication in cultured granulosa cells. *Proc Natl Acad Sci USA* 78(5):3000–3004.
38. Niwa H, Yamamura K, Miyazaki J (1991) Efficient selection for high-expression transfectants with a novel eukaryotic vector. *Gene* 108(2):193–199.
39. Liu K, Czaja MJ (2013) Regulation of lipid stores and metabolism by lipophagy. *Cell Death Differ* 20(1):3–11.
40. Hale AN, Ledbetter DJ, Gawriluk TR, Rucker EB, 3rd (2013) Autophagy: Regulation and role in development. *Autophagy* 9(7):951–972.
41. Ost A, et al. (2010) Attenuated mTOR signaling and enhanced autophagy in adipocytes from obese patients with type 2 diabetes. *Mol Med* 16(7-8):235–246.
42. van Zutphen T, et al. (2014) Lipid droplet autophagy in the yeast Saccharomyces cerevisiae. *Mol Biol Cell* 25(2):290–301.
43. Wang C, Liu Z, Huang X (2012) Rab32 is important for autophagy and lipid storage in Drosophila. *PLoS ONE* 7(2):e32086.
44. Lapierre LR, et al. (2013) Autophagy genes are required for normal lipid levels in C. elegans. *Autophagy* 9(3):278–286.
45. Ro SH, et al. (2013) Distinct functions of Ulk1 and Ulk2 in the regulation of lipid metabolism in adipocytes. *Autophagy* 9(12):2103–2114.
46. Brown MS, Goldstein JL (1980) Multivalent feedback regulation of HMG CoA reductase, a control mechanism coordinating isoprenoid synthesis and cell growth. *J Lipid Res* 21(5):505–517.
47. Chang TY, Chang CC, Cheng D (1997) Acyl-coenzyme A:cholesterol acyltransferase. *Annu Rev Biochem* 66:613–638.
48. Yang T, et al. (2002) Crucial step in cholesterol homeostasis: Sterols promote binding of SCAP to INSIG-1, a membrane protein that facilitates retention of SREBPs in ER. *Cell* 110(4):489–500.
49. Brown MS, Anderson RG, Goldstein JL (1983) Recycling receptors: The round-trip itinerary of migrant membrane proteins. *Cell* 32(3):663–667.
50. Röhrl C, Stangl H (2013) HDL endocytosis and resecretion. *Biochim Biophys Acta* 1831(11):1626–1633.
51. Thoresen SB, Pedersen NM, Liestøl K, Stenmark H (2010) A phosphatidylinositol 3-kinase class III sub-complex containing VPS15, VPS34, Beclin 1, UVRAG and BIF-1 regulates cytokinesis and degradative endocytic traffic. *Exp Cell Res* 316(20): 3368–3378.
52. Liang C, et al. (2008) Beclin1-binding UVRAG targets the class C Vps complex to coordinate autophagosome maturation and endocytic trafficking. *Nat Cell Biol* 10(7): 776–787.
53. Juhász G, et al. (2008) The class III PI(3)K Vps34 promotes autophagy and endocytosis but not TOR signaling in Drosophila. *J Cell Biol* 181(4):655–666.
54. Ruck A, et al. (2011) The Atg6/Vps30/Beclin 1 ortholog BEC-1 mediates endocytic retrograde transport in addition to autophagy in C. elegans. *Autophagy* 7(4):386–400.
55. Petiot A, Faure J, Stenmark H, Gruenberg J (2003) PI3P signaling regulates receptor sorting but not transport in the endosomal pathway. *J Cell Biol* 162(6):971–979.
56. Johnson EE, Overmeyer JH, Gunning WT, Maltese WA (2006) Gene silencing reveals a specific function of hVps34 phosphatidylinositol 3-kinase in late versus early endosomes. *J Cell Sci* 119(Pt 7):1219–1232.
57. Choi J, Jo M, Lee E, Choi D (2011) Induction of apoptotic cell death via accumulation of autophagosomes in rat granulosa cells. *Fertil Steril* 95(4):1482–1486.
58. Choi JY, Jo MW, Lee EY, Yoon BK, Choi DS (2010) The role of autophagy in follicular development and atresia in rat granulosa cells. *Fertil Steril* 93(8):2532–2537.
59. Peluso JJ, England-Charlesworth C, Bolender DL, Steger RW (1980) Ultrastructural alterations associated with the initiation of follicular atresia. *Cell Tissue Res* 211(1): 105–115.
60. Rosales-Torres AM, et al. (2000) Multiparametric study of atresia in ewe antral follicles: Histology, flow cytometry, internucleosomal DNA fragmentation, and lysosomal enzyme activities in granulosa cells and follicular fluid. *Mol Reprod Dev* 55(3): 270–281.
61. Rodgers RJ, Irving-Rodgers HF (2010) Morphological classification of bovine ovarian follicles. *Reproduction* 139(2):309–318.
62. Santos HB, et al. (2008) Ovarian follicular atresia is mediated by heterophagy, autophagy, and apoptosis in Prochilodus argenteus and Leporinus taeniatus (Teleostei: Characiformes). *Theriogenology* 70(9):1449–1460.
63. Kovács J, Forgó V, Péczely P (1992) The fine structure of the follicular cells in growing and atretic ovarian follicles of the domestic goose. *Cell Tissue Res* 267(3):561–569.
64. D'Herde K, De Prest B, Roels F (1996) Subtypes of active cell death in the granulosa of ovarian atretic follicles in the quail (Coturnix coturnix japonica). *Reprod Nutr Dev* 36(2):175–189.
65. Duerrschmidt N, et al. (2006) Lectin-like oxidized low-density lipoprotein receptor-1-mediated autophagy in human granulosa cells as an alternative of programmed cell death. *Endocrinology* 147(8):3851–3860.
66. Quatacker JR (1971) Formation of autophagic vacuoles during human corpus luteum involution. *Z Zellforsch Mikrosk Anat* 122(4):479–487.
67. Paavola LG (1977) The corpus luteum of the guinea pig. Fine structure at the time of maximum progesterone secretion and during regression. *Am J Anat* 150(4):565–603.
68. Paavola LG (1978) The corpus luteum of the guinea pig. III. Cytochemical studies on the Golgi complex and GERL during normal postpartum regression of luteal cells, emphasizing the origin of lysosomes and autophagic vacuoles. *J Cell Biol* 79(1):59–73.
69. Vanlennep EW, Madden LM (1965) Electron microscopic observations on the involution of the human corpus luteum of menstruation. *Z Zellforsch Mikrosk Anat* 66(3):365–380.
70. Bulling A, et al. (2000) Identification of an ovarian voltage-activated Na+-channel type: Hints to involvement in luteolysis. *Mol Endocrinol* 14(7):1064–1074.
71. Gaytán M, Morales C, Sánchez-Criado JE, Gaytán F (2008) Immunolocalization of beclin 1, a bcl-2-binding, autophagy-related protein, in the human ovary: Possible relation to life span of corpus luteum. *Cell Tissue Res* 331(2):509–517.
72. Ryter SW, Cloonan SM, Choi AM (2013) Autophagy: A critical regulator of cellular metabolism and homeostasis. *Mol Cells* 36(1):7–16.
73. Li WR, et al. (2011) Autophagic deficiency is related to steroidogenic decline in aged rat Leydig cells. *Asian J Androl* 13(6):881–888.
74. Binart N, Bachelot A, Bouilly J (2010) Impact of prolactin receptor isoforms on reproduction. *Trends Endocrinol Metab* 21(6):362–368.
75. Colosi P, et al. (1988) Biological, immunological, and binding properties of recombinant mouse placental lactogen-I. *Endocrinology* 123(6):2662–2667.
76. Soares MJ, Colosi P, Talamantes F (1982) The development and characterization of a homologous radioimmunoassay for mouse placental lactogen. *Endocrinology* 110(2):668–670.
77. Le JA, et al. (2012) Generation of mice expressing only the long form of the prolactin receptor reveals that both isoforms of the receptor are required for normal ovarian function. *Biol Reprod* 86(3):86.
78. Halperin J, et al. (2008) Prolactin signaling through the short form of its receptor represses forkhead transcription factor FOXO3 and its target gene galt causing a severe ovarian defect. *Mol Endocrinol* 22(2):513–522.
79. Caron KM, et al. (1997) Targeted disruption of the mouse gene encoding steroidogenic acute regulatory protein provides insights into congenital lipoid adrenal hyperplasia. *Proc Natl Acad Sci USA* 94(21):11540–11545.
80. Lucin KM, et al. (2013) Microglial beclin 1 regulates retromer trafficking and phagocytosis and is impaired in Alzheimer's disease. *Neuron* 79(5):873–886.
81. Beck S, et al. (2010) The worldwide incidence of preterm birth: A systematic review of maternal mortality and morbidity. *Bull World Health Organ* 88(1):31–38.
82. Shapiro-Mendoza CK, Lackritz EM (2012) Epidemiology of late and moderate preterm birth. *Semin Fetal Neonatal Med* 17(3):120–125.
83. Dudley DJ, Chen CL, Branch DW, Hammond E, Mitchell MD (1993) A murine model of preterm labor: Inflammatory mediators regulate the production of prostaglandin E2 and interleukin-6 by murine decidua. *Biol Reprod* 48(1):33–39.
84. Salo AL, Randall CL, Becker HC (1996) Effect of acute ethanol and cocaine administration on gestation days 14-17 in mice. *Alcohol* 13(4):369–375.
85. Dudley DJ, Branch DW, Edwin SS, Mitchell MD (1996) Induction of preterm birth in mice by RU486. *Biol Reprod* 55(5):992–995.
86. Udy GB, et al. (1997) Requirement of STAT5b for sexual dimorphism of body growth rates and liver gene expression. *Proc Natl Acad Sci USA* 94(14):7239–7244.
87. Teglund S, et al. (1998) Stat5a and Stat5b proteins have essential and nonessential, or redundant, roles in cytokine responses. *Cell* 93(5):841–850.
88. Wang H, Xie H, Dey SK (2008) Loss of cannabinoid receptor CB1 induces preterm birth. *PLoS ONE* 3(10):e3320.
89. Hirota Y, et al. (2010) Uterine-specific p53 deficiency confers premature uterine senescence and promotes preterm birth in mice. *J Clin Invest* 120(3):803–815.
90. Conde-Agudelo A, et al. (2013) Vaginal progesterone vs. cervical cerclage for the prevention of preterm birth in women with a sonographic short cervix, previous preterm birth, and singleton gestation: A systematic review and indirect comparison metaanalysis. *Am J Obstet Gynecol* 208(1):42 e41–42 e18.
91. Rode L, et al. (2009) Systematic review of progesterone for the prevention of preterm birth in singleton pregnancies. *Acta Obstet Gynecol Scand* 88(11):1180–1189.
92. Hassan SS, et al. (2011) Vaginal progesterone reduces the rate of preterm birth in women with a sonographic short cervix: A multicenter, randomized, double-blind, placebo-controlled trial. *Ultrasound Obstet Gynecol* 38(1):18–31.
93. Albrecht ED, Pepe GJ (1990) Placental steroid hormone biosynthesis in primate pregnancy. *Endocr Rev* 11(1):124–150.
94. Hung TH, Hsieh TT, Chen SF, Li MJ, Yeh YL (2013) Autophagy in the human placenta throughout gestation. *PLoS ONE* 8(12):e83475.